

## Wide-range temperature dependences of Brillouin scattering properties in polymer optical fiber

Kazunari Minakawa, Neisei Hayashi, Yuri Shinohara, Masaki Tahara, Hideki Hosoda, Yosuke Mizuno, and Kentaro Nakamura

Precision and Intelligence Laboratory, Tokyo Institute of Technology, Yokohama 226-8503, Japan

Received October 31, 2013; accepted February 16, 2014; published online March 27, 2014

We investigate the temperature dependences of the Brillouin scattering properties in a perfluorinated graded-index (PFGI-) polymer optical fiber (POF) in a wide temperature range from  $-160$  to  $125$  °C. The temperature dependences of the Brillouin frequency shift, linewidth, and Stokes power are almost linear at lower temperature down to  $-160$  °C; while they show nonlinear dependences at higher temperature. These behaviors appear to originate from the partial glass transition of the polymer material. © 2014 The Japan Society of Applied Physics

### 1. Introduction

Fiber-optic distributed temperature sensing has been demonstrated based on a number of principles including fiber Bragg gratings (FBGs),<sup>1-3</sup> Rayleigh scattering,<sup>4</sup> Raman scattering,<sup>5,6</sup> Brillouin scattering,<sup>7-11</sup> etc. Among them, Brillouin-based techniques have recently attracted significant attention because of their capability of distributed temperature and/or strain sensing on the basis of frequency information leading to high measurement stability.<sup>12-14</sup> Conventionally, their sensing heads were mainly composed of glass optical fibers such as silica glass fibers,<sup>7-14</sup> tellurite glass fibers,<sup>15</sup> bismuth-oxide glass fibers,<sup>15</sup> and photonic crystal fibers,<sup>16</sup> all of which are so fragile that they cannot withstand strains of over several percent. To enhance the limitation of the measurable strain, we have been studying the sensor applications of Brillouin scattering in polymer optical fibers (POFs),<sup>17-21</sup> which are sufficiently flexible to withstand strains of up to 50%.<sup>21</sup>

Up to now, Brillouin scattering in perfluorinated graded-index (PFGI-) POFs have been successfully observed at  $1.55$   $\mu\text{m}$ <sup>19</sup> and its sensing characteristics have been clarified, which include the Brillouin frequency shift (BFS) dependences on strain (relatively small strains from 0 to 1%,<sup>20</sup> and large strains of up to  $\sim 20\%$ <sup>21</sup>) and temperature (relatively narrow range from 30 to 80 °C<sup>20</sup>). However, the wide-range temperature dependences of the Brillouin scattering properties in POFs have not been reported yet, which are extremely important for their practical applications to temperature sensing in cryogenic or high-temperature environments.

In this study, we fully investigate the temperature dependences of the Brillouin scattering properties, i.e., the BFS, linewidth, and Stokes power, in a PFGI-POF in a wide temperature range from  $-160$  to  $125$  °C. Although the temperature dependences of these three parameters are almost linear at lower temperature down to  $-160$  °C, they are found to be nonlinear at higher temperature of over  $\sim 80$  °C. These behaviors appear to originate from the low glass-transition temperature of the polymer that constitutes the POF. Our results indicate that the Brillouin scattering in PFGI-POFs can be exploited to perform cryogenic-temperature sensing as well as higher-temperature sensing.

### 2. Principle

When pump light is injected into an optical fiber, back-scattered light called Stokes light is generated due to the

interaction with acoustic phonons, and it propagates in the direction opposite to the pump light. This phenomenon is known as Brillouin scattering,<sup>12</sup> and the Stokes light spectrum is called the Brillouin gain spectrum (BGS). The center frequency of the BGS is known to be downshifted from that of the pump light by the amount called the BFS  $\nu_B$ , which is given as<sup>12</sup>

$$\nu_B = \frac{2nv_A}{\lambda}, \quad (1)$$

where  $n$  is the core refractive index,  $v_A$  is the acoustic velocity in the fiber, and  $\lambda$  is the pump wavelength.

If temperature change (or strain) is applied to the fiber, the BFS shifts toward higher or lower frequency depending on the fiber core material, which is the basic principle of fiber-optic Brillouin sensing. The BFS dependence on temperature has been investigated for many kinds of optical glass fibers, which include silica single-mode fibers (SMFs;  $+1.18$  MHz/K<sup>13</sup>), tellurite glass fibers ( $-1.14$  MHz/K<sup>15</sup>), bismuth-oxide glass fibers ( $-0.88$  MHz/K<sup>15</sup>), and germanium-doped PCFs ( $+0.82$  MHz/K) (all the coefficients described here have been recalculated using Eq. (1) under the assumption that the wavelength of the pump light is  $1.55$   $\mu\text{m}$  and that  $n$  is not dependent on the wavelength). The coefficient of the temperature dependence of the BFS in a PFGI-POF has also been clarified to be  $-4.09$  MHz/K,<sup>20</sup> but only in the temperature range of 30 to 80 °C. As for silica SMFs, the dependences of the Brillouin properties on extremely low temperature (down to 1.4 K) have been reported.<sup>22</sup>

The Stokes power as well as the BFS is also temperature-dependent; for example, the Stokes power in a silica SMF is reported to be enhanced with increasing temperature.<sup>23</sup> The Stokes power or the Brillouin gain coefficient is influenced by many structural quantities,<sup>12</sup> one of which is the effective length  $L_{\text{eff}}$  defined as

$$L_{\text{eff}} = \frac{1 - e^{-\alpha L}}{\alpha}, \quad (2)$$

where  $\alpha$  is the propagation loss and  $L$  is the fiber length.

### 3. Experimental methods

We employed an 8-m-long PFGI-POF as a sample, which consists of a core (50  $\mu\text{m}$  diameter), cladding (100  $\mu\text{m}$  diameter), and overcladding (750  $\mu\text{m}$  diameter) encased in polyvinyl chloride. The core and cladding layers are composed of doped and undoped polyperfluorobutylvinyl

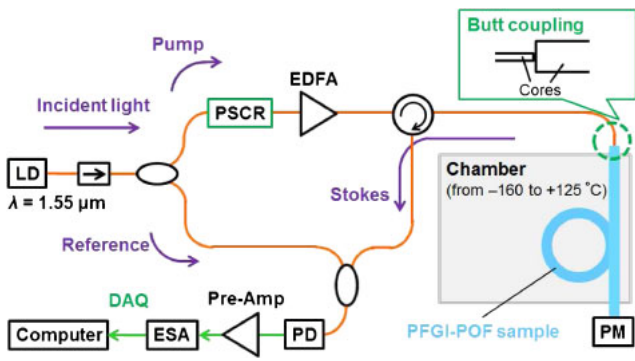


**Fig. 1.** (Color online) Experimental setup for observing Brillouin scattering in the PFGI-POF sample: DAQ, data acquisition; LD, laser diode; EDFA, erbium-doped fiber amplifier; ESA, electrical spectrum analyzer; PD, photo-diode; PM, powermeter; PSCR, polarization scrambler.

ether, respectively. It has a numerical aperture (NA) of 0.185, a core refractive index of  $\sim 1.35$ , a propagation loss of  $\sim 250$  dB/km at  $1.55 \mu\text{m}$ , and a core glass-transition temperature of  $< 108^\circ\text{C}$ . According to the specification sheet provided by the manufacturer, this POF is suitable for telecom use only in the temperature range from  $0$  to  $70^\circ\text{C}$  because of the increased loss.

The experimental setup shown in Fig. 1 was basically the same as that previously reported,<sup>19)</sup> where self-heterodyne detection was utilized for high-resolution monitoring of the BGS. The laser wavelength was  $1.55 \mu\text{m}$ , and the POF sample was placed in a thermostatic chamber. The pump power injected into the sample was fixed at  $20 \text{ dBm}$  ( $= 100 \text{ mW}$ ), and the influence of the polarization state was mitigated using a polarization scrambler.

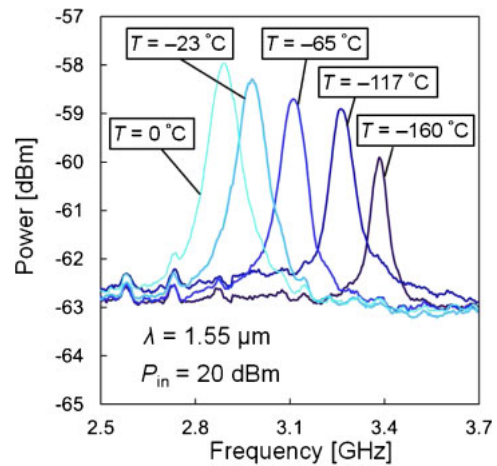
#### 4. Experimental results

##### 4.1 Brillouin gain spectrum

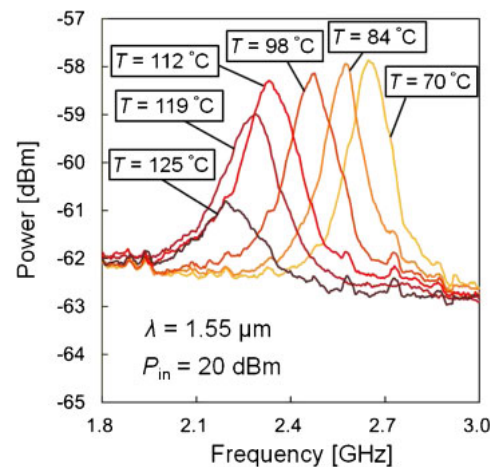
After being set to  $-160^\circ\text{C}$ , the temperature was gradually raised. Figure 2(a) shows the measured BGS dependence on low temperature from  $-160$  to  $0^\circ\text{C}$ . With increasing temperature from  $-160^\circ\text{C}$ , the BGS shifted to lower frequency, and the Stokes power was raised. Figure 2(b) shows the measured BGS dependence on relatively high temperature from  $70$  to  $125^\circ\text{C}$ . As the temperature was increased, the BGS shifted to lower frequency; the Brillouin linewidth was broadened and the Stokes power was reduced.

##### 4.2 Brillouin frequency shift

From Fig. 2, we can extract the detailed temperature dependences of the BFS, linewidth, and Stokes power. Figure 3 shows the BFS dependence on wide-range temperature from  $-160$  to  $125^\circ\text{C}$ , which was obtained by fitting each BGS with a Lorentzian curve. In the temperature range below  $\sim 85^\circ\text{C}$ , the dependence was linear with no hysteresis. The slope was about  $-3.2 \text{ MHz/K}$ , which is smaller than that of our previous report.<sup>20)</sup> This discrepancy seems to be caused by the differences in material and structure of the POFs. At  $> 85^\circ\text{C}$ , the slope became steeper, reaching  $-13.8 \text{ MHz/K}$  at  $125^\circ\text{C}$ . Considering that the glass-transition temperature of the core material is  $< 108^\circ\text{C}$ , this nonlinear behavior is probably due to the change in physical properties of the softened core. After being kept at  $125^\circ\text{C}$  for  $5 \text{ min}$ , the temperature was decreased, during which the BFS was reduced



(a)



(b)

**Fig. 2.** (Color online) Measured dependence of the BGS on (a) low temperature from  $0$  to  $-160^\circ\text{C}$  and (b) higher temperature from  $70$  to  $125^\circ\text{C}$ .

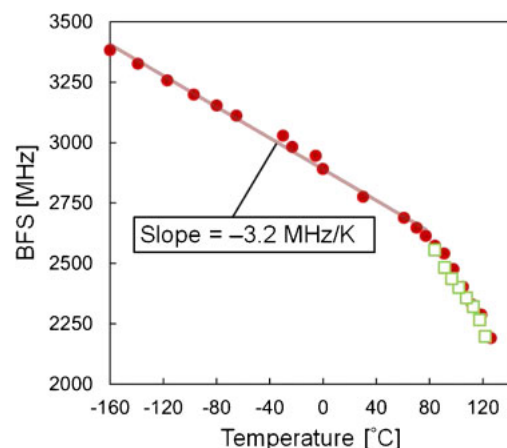


**Fig. 3.** (Color online) Temperature dependence of the BFS. The solid circles and the open squares indicate the measured points with increasing temperature from  $-160^\circ\text{C}$  and with decreasing temperature from  $125^\circ\text{C}$ , respectively.

with no hysteresis. The BGS was buried by the noise floor at  $\sim 80^\circ\text{C}$ , and the BFS was no longer measurable. This result indicates that highly-sensitive temperature sensing based

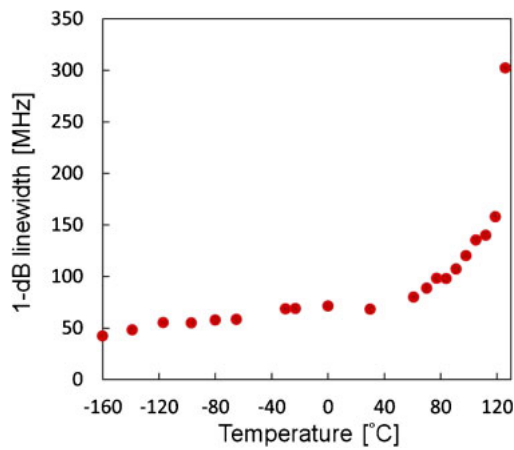


Fig. 4. (Color online) Temperature dependence of the 1-dB Brillouin linewidth.

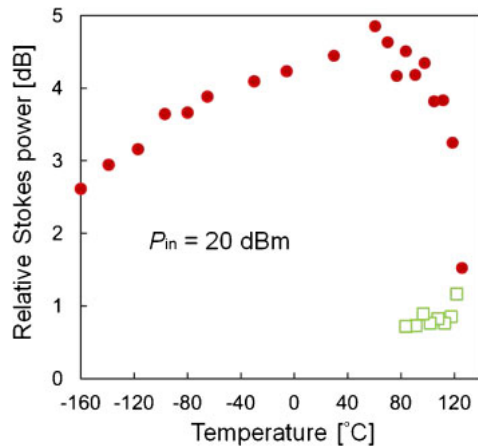
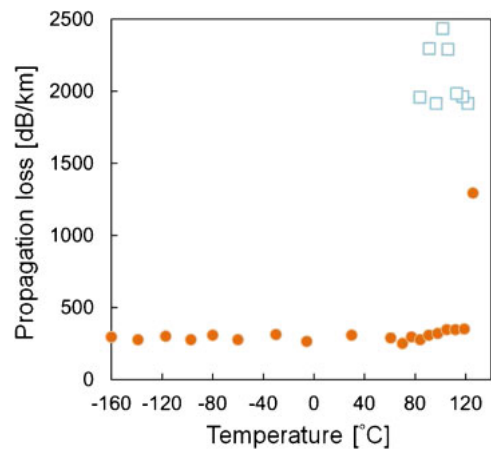


Fig. 5. (Color online) Temperature dependence of the Stokes power. The solid circles and the open squares indicate the measured points with increasing temperature from  $-160\text{ }^{\circ}\text{C}$  and with decreasing temperature from  $125\text{ }^{\circ}\text{C}$ , respectively.

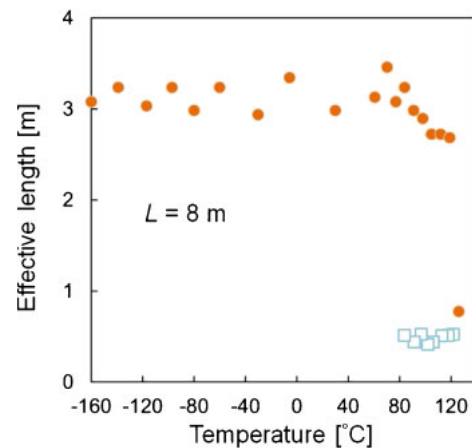
on Brillouin scattering in PFGI-POFs is feasible in the wide temperature range including cryogenic temperature. The nonlinear behavior of the BFS at higher temperature is physically interesting, and could be exploited to enhance the measurement sensitivity in future.

### 4.3 Brillouin linewidth

Next, the temperature dependence of the Brillouin linewidth was plotted as shown in Fig. 4. Since the Stokes power was not sufficiently high compared with the noise floor, we utilized not 3-dB but 1-dB linewidth. While the temperature was being raised from  $-160\text{ }^{\circ}\text{C}$ , the linewidth was gradually increased. The sign of this dependence was the opposite of that of silica SMFs,<sup>23)</sup> either because of the phonon absorption peak<sup>23)</sup> in the POF at high temperature or because of the multimode nature of the POF. The increase in the linewidth became drastic at  $>70\text{ }^{\circ}\text{C}$ , apparently caused by the gradual glass transition of the core that reduces the uniformity of the fiber cross-section. Note that the linewidth at  $125\text{ }^{\circ}\text{C}$  was not fairly estimated, because the Stokes power was extremely low (as is discussed in the next section).



(a)



(b)

Fig. 6. (Color online) Temperature dependences of (a) the propagation loss and (b) the effective length of the POF. The solid circles and the open squares indicate the measured points with increasing temperature from  $-160\text{ }^{\circ}\text{C}$  and with decreasing temperature from  $125\text{ }^{\circ}\text{C}$ , respectively.

### 4.4 Stokes power

Finally, the temperature dependence of the Stokes power is shown in Fig. 5. As the temperature was raised from  $-160\text{ }^{\circ}\text{C}$ , the Stokes power was gradually increased and reached its maximum at  $\sim 60\text{ }^{\circ}\text{C}$ . This behavior is the same as that of silica SMFs.<sup>23)</sup> However, as the temperature was further raised, the Stokes power started to decrease; at  $>120\text{ }^{\circ}\text{C}$ , the decrease became drastic. When the temperature was lowered after being kept at  $125\text{ }^{\circ}\text{C}$  for 5 min, the Stokes power was no longer restored to the initial value.

In order to clarify the reason for the behavior at higher temperature, the temperature dependence of the propagation loss of the POF was measured, as shown in Fig. 6(a). The loss was almost constant in the temperature range from  $-160$  to  $120\text{ }^{\circ}\text{C}$ , but it abruptly started to increase at  $>120\text{ }^{\circ}\text{C}$  never to return to the initial value by decreasing the temperature later. The temperature dependence of the Brillouin effective length  $L_{\text{eff}}$  calculated using Eq. (2) is also shown in Fig. 6(b), the trend of which is quite similar to Fig. 5 at  $>60\text{ }^{\circ}\text{C}$ . Thus, we may naturally consider that the hysteresis of the Stokes power is caused by the destroyed wave-guiding structure (core and cladding) owing to the partial glass transition of the polymer material.

## 5. Conclusions

The temperature dependences of the Brillouin scattering properties such as the BFS, linewidth, and Stokes power, in a PFGI-POF were investigated in a wide temperature range from  $-160$  to  $125$  °C. Although the temperature dependences of these three parameters can be regarded as almost linear at lower temperature down to  $-160$  °C, they are found to be nonlinear at higher temperature of over  $\sim 80$  °C. The Stokes power displayed a hysteresis characteristic at  $\sim 125$  °C. These behaviors seem to originate from the partial glass transition of the core material of the POF. Brillouin scattering in PFGI-POFs can be expected from our results to have a big potential for cryogenic-temperature sensing as well as higher-temperature sensing.

## Acknowledgements

The authors wish to thank Dr. Kotaro Koike (Keio Photonics Research Institute, Keio University) for his helpful comments. This work was partially supported by a Grant-in-Aid for Young Scientists (A) (No. 25709032) from the Japan Society for the Promotion of Science (JSPS) and by research grants from the General Sekiyu Foundation, the Iwatani Naoji Foundation, and the SCAT Foundation. N.H. acknowledges a Grant-in-Aid for JSPS Fellows (No. 25007652).

- 1) K. O. Hill, Y. Fujii, D. C. Johnson, and B. S. Kawasaki, *Appl. Phys. Lett.* **32**, 647 (1978).
- 2) P. C. Won, J. Leng, Y. Lai, and J. A. R. Williams, *Meas. Sci. Technol.* **15**, 1501 (2004).
- 3) K. Hotate and K. Kajiwara, *Opt. Express* **16**, 7881 (2008).
- 4) A. Hartog, *J. Lightwave Technol.* **1**, 498 (1983).
- 5) M. A. Farahani and T. Gogolla, *J. Lightwave Technol.* **17**, 1379 (1999).
- 6) J. P. Dakin, D. J. Pratt, G. W. Bibby, and J. N. Ross, *Electron. Lett.* **21**, 569 (1985).
- 7) T. Horiguchi and M. Tateda, *J. Lightwave Technol.* **7**, 1170 (1989).
- 8) D. Garus, K. Krebber, F. Schliep, and T. Gogolla, *Opt. Lett.* **21**, 1402 (1996).
- 9) K. Hotate and T. Hasegawa, *IEICE Trans. Electron.* **E83-C**, 405 (2000).
- 10) T. Kurashima, T. Horiguchi, H. Izumita, S. Furukawa, and Y. Koyamada, *IEICE Trans. Commun.* **E76-B**, 382 (1993).
- 11) Y. Mizuno, W. Zou, Z. He, and K. Hotate, *Opt. Express* **16**, 12148 (2008).
- 12) G. P. Agrawal, *Nonlinear Fiber Optics* (Academic, San Diego, CA, 1995).
- 13) T. Kurashima, T. Horiguchi, and M. Tateda, *Appl. Opt.* **29**, 2219 (1990).
- 14) T. Horiguchi, T. Kurashima, and M. Tateda, *IEEE Photonics Technol. Lett.* **1**, 107 (1989).
- 15) Y. Mizuno, Z. He, and K. Hotate, *Appl. Phys. Express* **2**, 112402 (2009).
- 16) L. Zou, X. Bao, S. Afshar, and L. Chen, *Opt. Lett.* **29**, 1485 (2004).
- 17) M. G. Kuzyk, *Polymer Fiber Optics: Materials, Physics, and Applications* (CRC Press, Boca Raton, FL, 2006).
- 18) Y. Koike and M. Asai, *NPG Asia Mater.* **1**, 22 (2009).
- 19) Y. Mizuno and K. Nakamura, *Appl. Phys. Lett.* **97**, 021103 (2010).
- 20) Y. Mizuno and K. Nakamura, *Opt. Lett.* **35**, 3985 (2010).
- 21) N. Hayashi, Y. Mizuno, and K. Nakamura, *Opt. Express* **20**, 21101 (2012).
- 22) S. Le Floch and P. Cambon, *Opt. Commun.* **219**, 395 (2003).
- 23) M. Nikles, L. Thevenaz, and P. A. Robert, *J. Lightwave Technol.* **15**, 1842 (1997).